NÖHÜ Müh. Bilim. Derg. / NOHU J. Eng. Sci., 2022; 11(3), 797-805

Niğde Ömer Halisdemir Üniversitesi Mühendislik Bilimleri Dergisi
Niğde Ömer Halisdemir University Journal of Engineering Sciences

Araştırma makalesi / Research article

www.dergipark.org.tr/tr/pub/ngumuh / www.dergipark.org.tr/en/pub/ngumuh

An investigation of the effect of tapered angle and boundary condition on natural frequency of different ceramic coated Ti-6Al-4V alloy with finite element analysis

Farklı seramik kaplı Ti-6Al-4V alaşımının doğal frekansına konik açı ve sınır koşulunun etkisinin sonlu eleman analizi ile incelenmesi

Berkay Ergene[1,*], Çağın Bolat[2]

[1] *Pamukkale University, Mechanical Engineering Department, 20160, Denizli, Turkey*
[2] *Istanbul Technical University, Mechanical Engineering Department, 34437, Istanbul, Turkey*

Abstract

In recent years, the interest in light metals has increased due to the increasing demand for components with high specific strength and long service life in the industry. In this context, titanium alloys have become very common and popular owing to their high strength/weight properties and superior refractory characteristics. In this study, the effect of boundary condition and tapered angle on the natural frequency and vibration behavior of the beam was investigated in Ti-6Al-4V beams coated with three different ceramic materials; Al_2O_3, AlN, and TiB_2. Tapered angle values are considered as 0°, 0.2°, 0.4°, 0.6° and 0.8°. Besides, boundary conditions were evaluated in two conditions including left side fixed or both sides fixed. All analyzes were performed in the finite element-based Ansys APDL 19 program. According to the results obtained from the analyses, it was observed that there was a change in the natural frequency values according to the type of coating material, but no difference was found in terms of increase/decrease tendency. In addition, the resultant displacement values were determined for all samples. The results indicated that the resultant displacement values were severely affected by the tapered angle. A decreasing resultant displacement trend was observed in all samples with increasing tapered angle.

Keywords: Natural frequency, Ceramic coating, Tapered beam, Vibration behavior, Ti-6Al-4V

Öz

Son yıllarda sektörde özgül mukavemeti yüksek ve uzun ömürlü bileşenlere olan talebin artması nedeniyle hafif metallere olan ilgi artmıştır. Bu bağlamda titanyum alaşımları, yüksek mukavemet/ağırlık özellikleri ve üstün refrakter özellikleri nedeniyle oldukça yaygın ve popüler hale gelmiştir. Bu çalışmada, Al_2O_3, AlN ve TiB_2 olmak üzere üç farklı seramik malzemesi ile kaplanmış Ti-6Al-4V kirişlerde sınır koşulunun ve konik açının kirişin doğal frekansı ve titreşim davranışına olan etkisi araştırılmıştır. Konik açı değerleri 0°, 0.2°, 0.4°, 0.6° ve 0.8° olarak ele alınmıştır. Ayrıca, sınır koşulları sol kenarın sabitlenmesi ya da her iki kenarın da sabitlenmesi olarak iki şekilde değerlendirilmiştir. Tüm analizler sonlu elemanlar bazlı Ansys APDL 19 programında gerçekleştirilmiştir. Analizlerden elde edilen sonuçlara göre, kaplama malzemesinin cinsine göre doğal frekans değerlerinde değişim olduğu ancak artış/azalma eğilimi açısından bir farklılık olmadığı görülmüştür. Ek olarak, tüm numuneler için bileşke deplasman değerleri belirlenmiştir. Sonuçlar, bileşke deplasman değerlerinin konik açıdan ciddi şekilde etkilendiğini göstermiştir. Konik açının artışı ile birlikte tüm numunelerin bileşke deplasman değerlerinde azalış eğilimi gözlemlenmiştir.

Anahtar kelimeler: Doğal frekans, Seramik kaplama, Konik kiriş, Titreşim davranışı, Ti-6Al-4V

1 Introduction

Light metals like magnesium, aluminum, and titanium have become popular in recent years due to the fact that they carry a promising potential for high specific mechanical properties. From the composite and foam industry to the medical and construction sector, many different usage areas can be counted for these metals depending on design requirements [1-5]. Owing to their low density and high strength combination, total interest in these classes of materials by researchers and engineers working on structural optimizations has started to rise nowadays [6, 7].

Ti-6Al-4V metallic alloy, which is also called Ti64, is a dual-phase ($\alpha+\beta$) titanium alloy and it exhibits sufficient yield strength, low density, good fracture toughness, and perfect corrosion resistance [8]. Thanks to its high specific mechanical responses, Ti-6Al-4V alloy has been used frequently by engineers in lots of critical structural parts such as gas turbines, jet engines, fuselage components, and airframe parts [9, 10]. Also, in comparison with the other alloys series of titanium, it is correct to allege that Ti-6Al-4V dominates the market sales since its appearing in the sector [11]. Weight reduction capacity, superior mechanical features, and excellent corrosion endurance are the most influential reasons behind this circumstance.

To date, there has been made lots of scholarly endeavors aiming to elucidate the mechanical and physical properties

* Sorumlu yazar / Corresponding author, e-posta / e-mail: bergene@pau.edu.tr (B. Ergene)
Geliş / Recieved: 24.02.2022 Kabul / Accepted: 06.05.2022 Yayımlanma / Published: 18.07.2022
doi: 10.28948/ngmuh.1078779

of Ti-6Al-4V alloys by various investigation teams. Nevertheless, these attempts have remained limited to elastic properties, plastic behaviors, wear resistance, fatigue, and corrosion potential [12-16]. Corrosion can be interpreted as a noteworthy problem for this kind of titanium alloy in industrial service conditions and can be prevented with some coating techniques. In the technical literature, some valuable efforts are present to emphasize the positive effect of the coating process. For instance, Hussain et al. [17] proposed poly (ε-caprolactone)/hydroxyapatite composite coating to block undesired corrosion in Ti-6Al-4V samples. Haider et al. [18] deposited graphene oxide film on Ti-6Al-4V samples and improved the corrosion resistance. Mordyuk et al. [19] reported that Al_2O_3 composite coatings could enhance the corrosion and oxidation properties of Ti-6Al-4V substrates. Mandal et al. [20] worked on hard AlN coatings and applied them to Ti-6Al-4V samples. The research group claimed that coated samples displayed better tribo-corrosion performance. Bolat et al. [21] pointed out that Al_2O_3, AlN, and TiB_2 coatings not only reflected better corrosion resistance for Ti-6Al-4V samples but they also provided sufficient elasticity under a load of thermal stresses. Lin et al. [22] offered TiN coatings on Ti-6Al-4V samples for longer service life under corrosive environments and utilized a multi arc-ion plating process for the manufacturing of the protective layer.

In the light of the previous scientific studies published in the technical archives, it can be put forward that there is a lack of interest in the topics of vibration properties of the coated Ti-6Al-4V alloy. Accordingly, if it is considered that all design components are subjected to vibrational effect in the real service conditions, it should be underlined that the correct detection of the natural frequency of the coated samples is notably significant. Thanks to true frequency predictions, unwanted separation of coating layers and severe damage of substrate material can be hindered. In this paper, three different hard ceramic coatings (Al_2O_3, AlN, and TiB_2) were selected and their effect on the natural frequency capacity of the Ti-6Al-4V was analyzed by using finite element methodology. All components were modeled using proper meshing models. According to the simulation results, all coating ceramics were compared to each other and some further recommendations were made.

2 Material and method

It is known that the natural frequency of the cantilever beam can be calculated with Equation 1 given below. In Equation 1, f_n, K_n, E, I, g, l and w demonstrate the natural frequency, constant where n refers to the mode of vibration, elasticity modulus, area moment of inertia, gravitational acceleration, length of the beam and uniform weight respectively [7].

$$f_n = \frac{K_n}{2\pi}\sqrt{\frac{EIg}{wl^4}} \tag{1}$$

In this study, Ti-6Al-4V beam models (with a length of 200 mm, a width of 20 mm, and, a thickness of 2 mm) were designed in Ansys APDL 19.0 finite element-based program as shown in Figure 1.

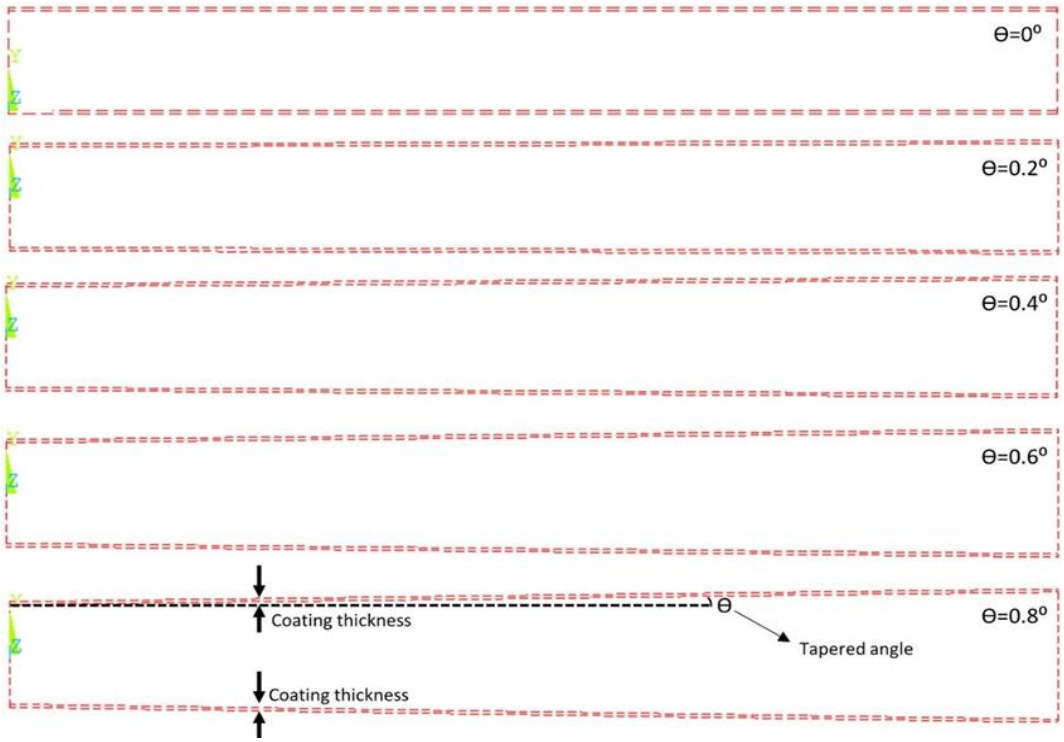

Figure 1. The view of the tapered angles (Θ) on the designed Ti-6Al-4V beams with coating thickness of 0,6 mm; Θ = 0º, Θ = 0.2º, Θ = 0.4º, Θ = 0.6º and Θ = 0.8º respectively

As coating ceramics, hard AlN, Al_2O_3, and TiB_2 were appointed and the coating thickness values were designated as 0.6 mm. During the modeling procedure, both beam and coating layer was created with different areas and then these areas were glued to each other to be able to define different material properties for the beam and coating layer. These three hard ceramics were selected since they have been used frequently by different investigators due to their high hardness and rigidity as composite reinforcements and coating layers [23-28]. Also, five different tapered angles were picked up in order to conceive the impact of the geometrical factor. In Table 1, material properties utilized in the Ansys APDL program can be followed easily.

Table 1. Material properties of base and coating materials [21]

Material Type	Elasticity Modulus (MPa)	Poisson's Ratio	Density (g/cm^3)
Ti-6Al-4V	110 000	0.310	4.41
AlN	341 000	0.240	3.26
Al_2O_3	403 000	0.210	3.95
TiB_2	562 000	0.108	4.52

Designed beams were subjected to homogenously meshing procedure with Quad 4 Node 182 element type with plane thickness option which has four nodes with two degrees of freedom at each node: translations in the nodal x and y directions [29]. In addition, two different test conditions in another name boundary conditions were adjusted. Firstly, the left end of the tapered beam was fixed as a boundary condition. Secondly, both design ends were fixed (Figure 2a). During the meshing procedure, firstly the total model was meshed with an element size of 0.1 mm, 0.2 mm, and 0.3 mm respectively, and solved. However, as a result of mesh optimization, it was observed that the obtained results differ for element sizes of 0.3 mm than others significantly and no remarkable difference was noted between element sizes of 0.2 mm and 0.1 mm. Therefore, to minimize the solution time, 0.2 mm element size was preferred and the total number of 136656 nodes and 135534 elements were generated. Meshed part can be seen in Figure 2b. What is more, modal analyses were conducted in the Block Lanczos module with active ten-mode. Thus, the first natural frequency of the coated tapered beams and occurred maximum resultant displacement values were obtained depending on coating materials, tapered angles and test conditions.

3 Finite element results

For the only left-side fixing condition (Condition 1), the results of the finite element analyses performed with the Ansys APDL 19 program are given in Figure 3 and Figure 4. Figure 3 shows how the type of coating material and the tapered angle of the beam affect the first natural frequency values of the beams.

In the case where the coating material is AlN, the highest first natural frequency occurred at 15.647 Hz when the tapered angle was 0.2º. On the other hand, the lowest first natural frequency value of 15.079 Hz was observed when the tapered angle was 0.8º. In case the tapered angle increases from 0º to 0.2º, an increase was observed in the first natural frequency value of the beam, while the first natural frequency values of the beam decrease when the tapered angle exceeded 0.2º (Figure 3a). In the case where the coating material is Al_2O_3, it was ascertained that the first natural frequency values of the beam escalated in a range of 2% to 3%, compared to the situation in Figure 3a. The highest first frequency value of 16.105 Hz and the lowest first natural frequency value of 15.498 Hz were found when the tapered angle values were 0.2° and 0.8° respectively (Figure 3b). Moreover, it can be noted that the first natural frequency values dropped slightly from 0.2° to 0.8°.

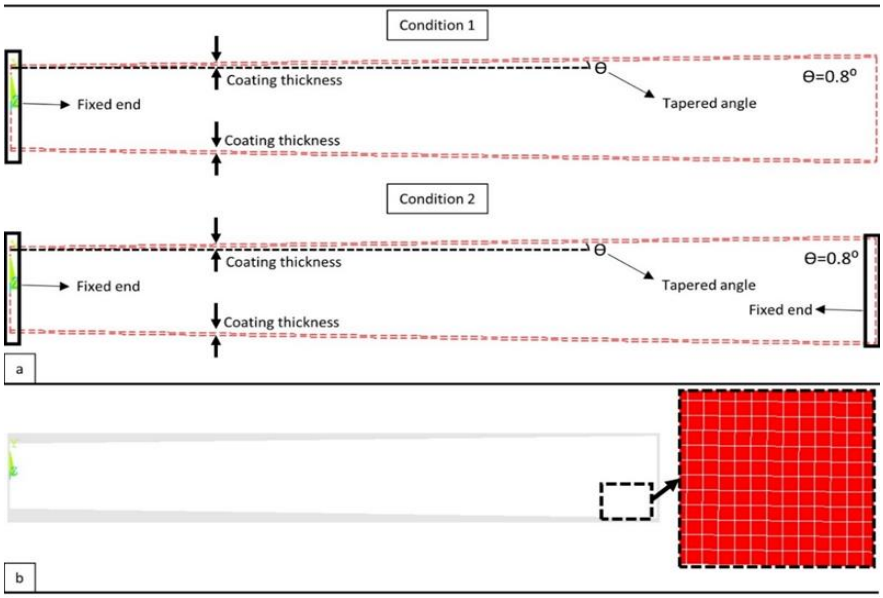

Figure 2. An illustrative view of the designed beams with boundary condition and mesh, a) View of the boundary conditions, b) view of the generated mesh

When the coating material type is TiB_2 (Figure 3c), the first natural frequency value reached its peak value of 17.313 Hz for a 0.2° tapered angle. On the other side, the minimum first natural value was detected as 16.596 Hz for the tapered angle of 0.8°. A similar declining trend that was noticed for other ceramic coating versions was seen for TiB_2 coated beams between 0.2° and 0.8° tapered angles.

If a general assessment is made with the finite analyses obtained, there is no inconvenience to state that the elastic modulus of the coating ceramics plays an important role in the natural frequency outcomes. In comparison with the other hard coatings, TiB_2 coatings had higher levels of frequency and this situation can be attributed to their higher elastic modulus of 562 GPa. Besides, for all kinds of coating types, it can be emphasized that the geometrical factor of the tapered angle also was effective for the natural frequency results. Regardless of the coating material, while a slight frequency increase is present between 0° and 0.2° tapered angle values, a decreasing tendency can be seen from 0.2° and 0.8° tapered angles.

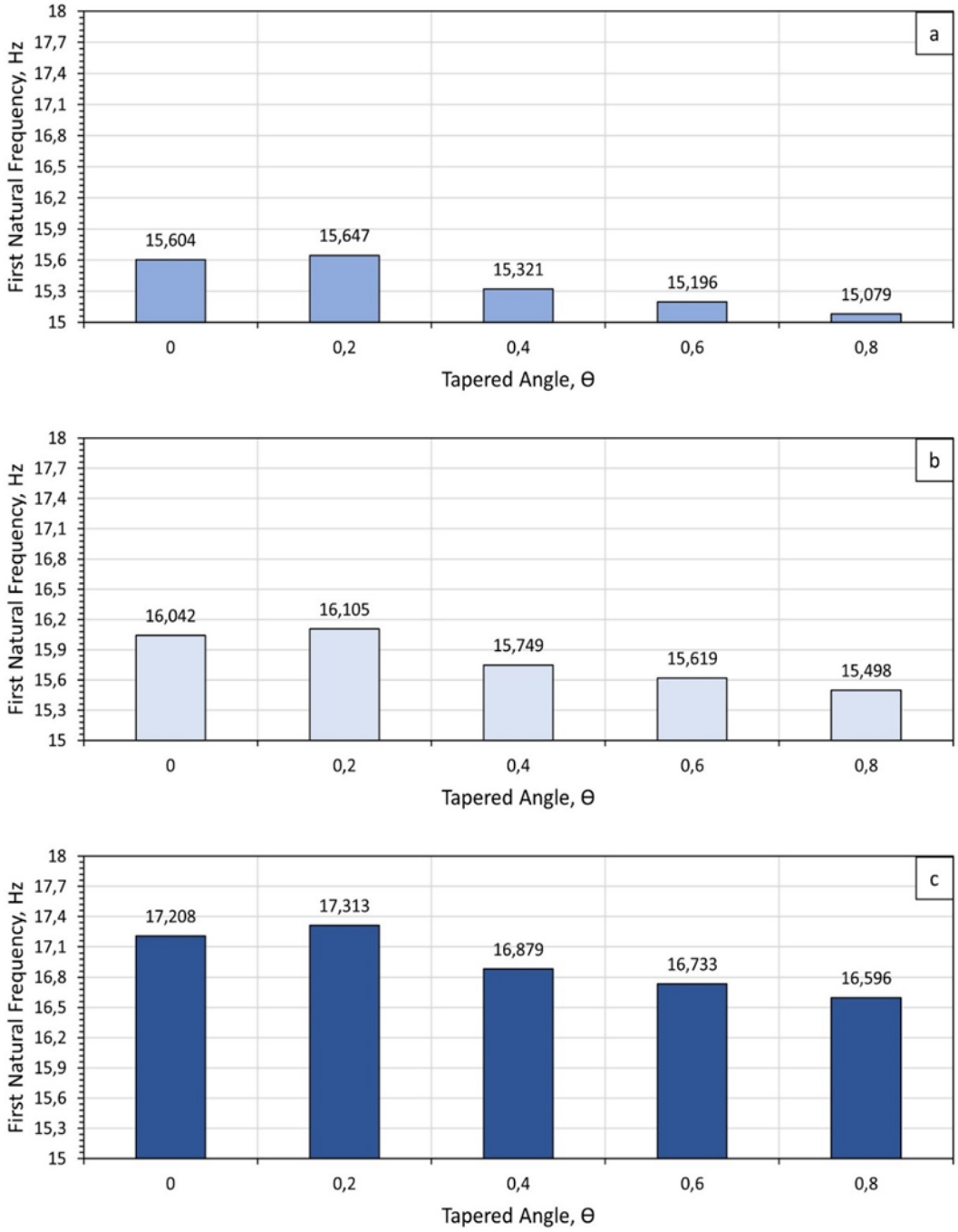

Figure 3. First natural frequency values of Ti-6Al-4V beams with different coatings depending on tapered angle for condition 1, a) AlN, b) Al_2O_3, c) TiB_2

Displacement analyses are considerably significant for the design requirements and physical stability of the coating material. Especially for hard and rigid ceramic coating layers, this factor must be taken into the account carefully. In Figure 4, the resultant displacement values of the coating materials are given based on the changing tapered angle values. In addition, it should be pointed out that the obtained displacement values from the finite element analyses can be considered as the relative values due to no acting force on the beams which leads to a deformation in the modal analysis. In Figure 4a, Figure 4b, and Figure 4c, the coating materials of the beams are AlN, Al_2O_3, and TiB_2, respectively. From Figure 4a, the resultant displacement values decrease with the increase of the tapered angle. According to the analyses, the highest and the lowest resultant displacement values were determined as 10.386 mm and 9.293 mm for AlN and TiB_2 coated beams respectively.

If the graph drawn in Figure 4b is examined, it is seen that the resultant displacement values have a decreasing trend. Similar to the trend in Figure 4a, a diminishment in the resultant displacement values was observed with the increase of the tapered angle in Figure 4b. For Al_2O_3 coated beams, the highest resultant displacement value was determined as 10.337 mm when the tapered angle was 0º, and the lowest resultant displacement value was determined as 9.258 mm when the tapered angle was 0.8°.

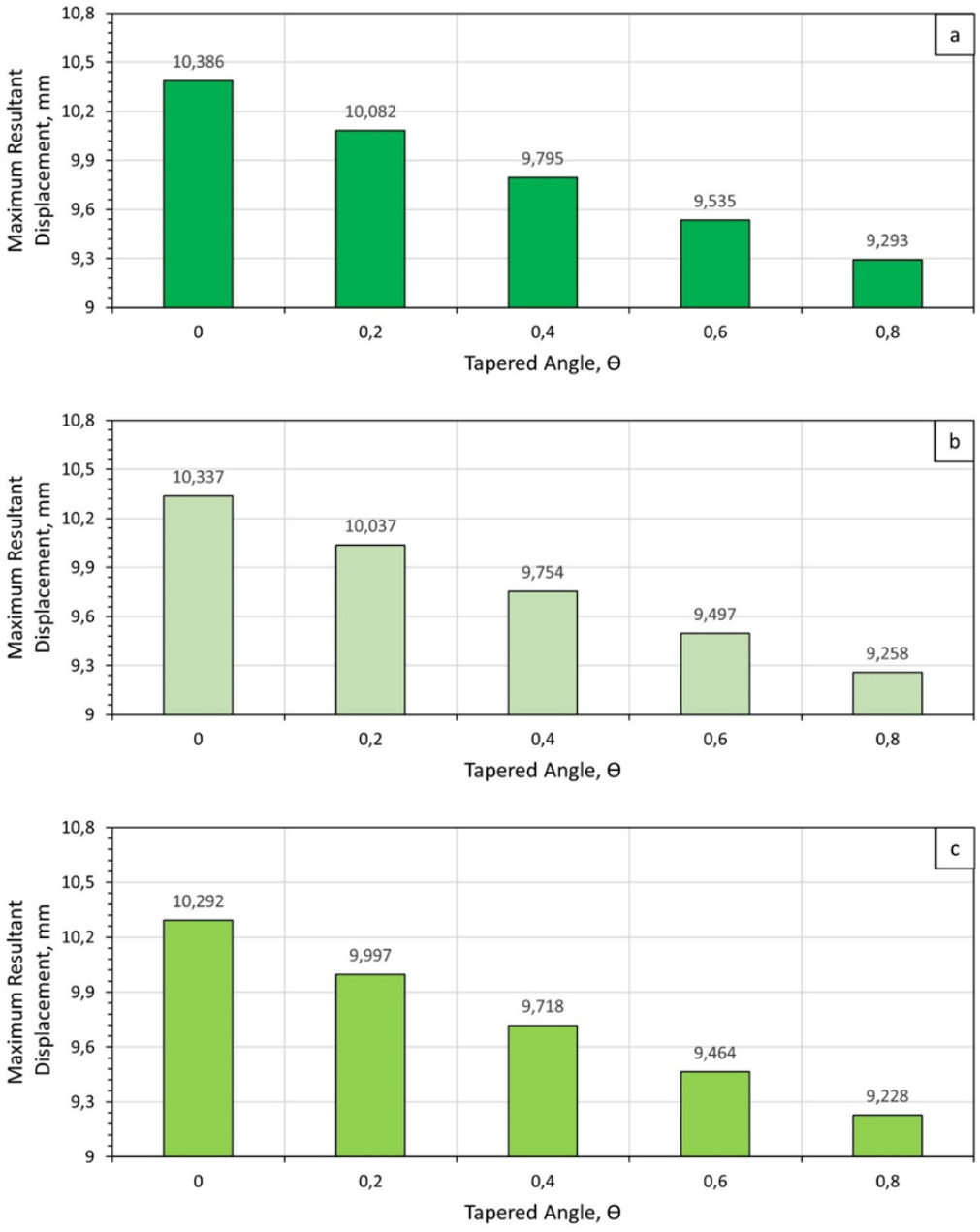

Figure 4. Maximum resultant displacement values of Ti-6Al-4V beams with different coatings depending on tapered angle for condition 1, a) AlN, b) Al_2O_3, c) TiB_2

In the case where the coating material is TiB_2, an apparent decrement was observed in the resultant displacement values similar to the other two cases. From Figure 4c, the highest and lowest resultant displacement values are 10.292 mm and 9.228 mm, respectively. At this point, it is also worth mentioning that when Figure 3 and Figure 4 are examined together, it can be reported that while the first natural frequency of the beam is high, the resulting resultant displacement value decreases. Furthermore, Figure 5 shows the simulation image of an analyzed sample (TiB_2 coated beam with tapered angle of 0.8°), and alike results were seen also for all kinds of coating types and tapered angles.

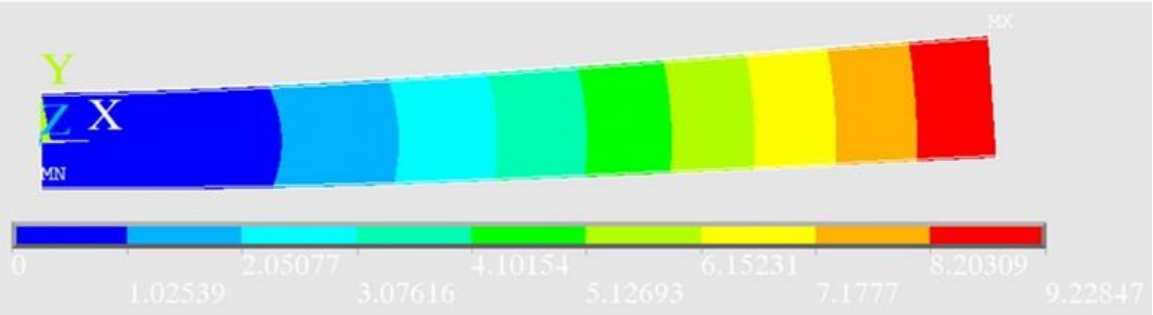

Figure 5. An illustrative example for vibrational behavior of the coated tapered beams at condition 1 (TiB_2 coated beam with tapered angle of 0.8°)

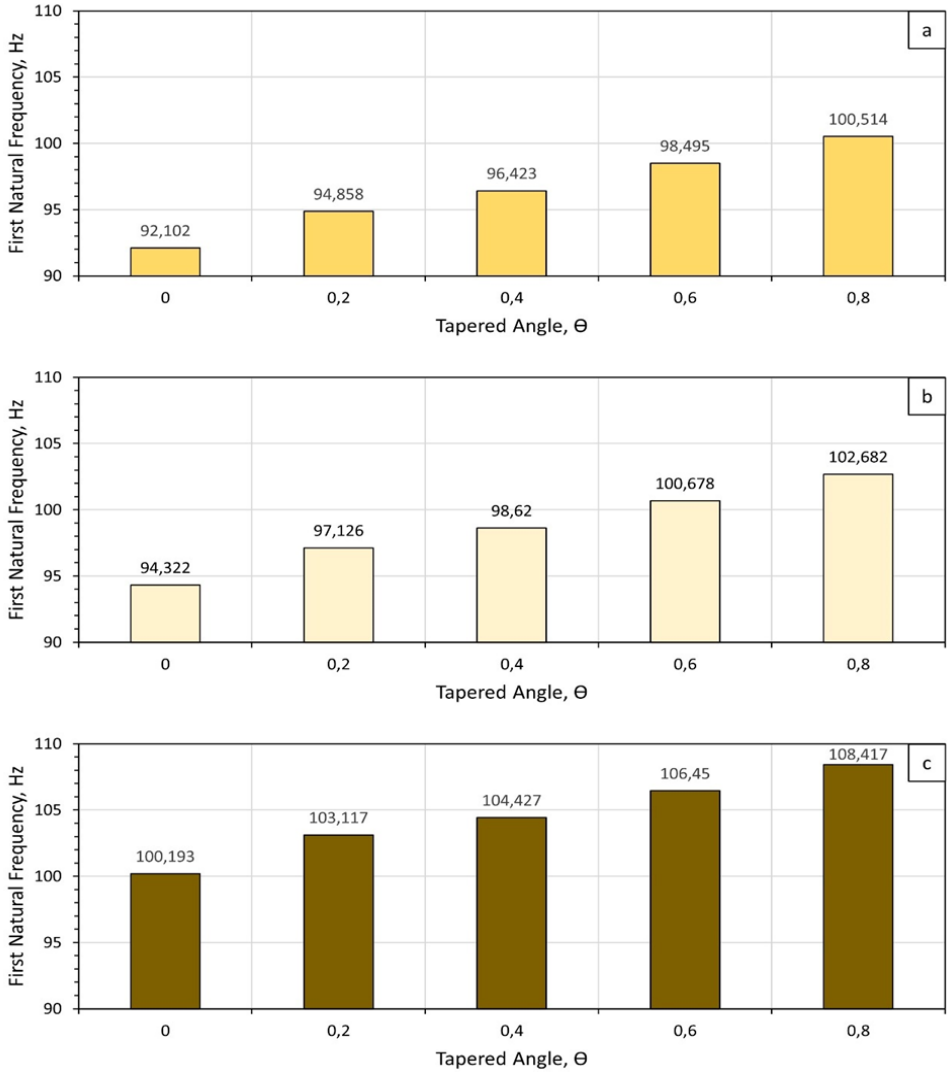

Figure 6. First natural frequency values of Ti-6Al-4V beams with different coatings depending on tapered angle for condition 2, a) AlN, b) Al_2O_3, c) TiB_2

For the two-side fixing condition, the results of the finite element analyses conducted with the Ansys APDL 19 software are shared in Figure 6 and Figure 7. In the case where the coating material is AlN, the maximum first natural frequency value was recorded as 100.514 Hz when the tapered angle was 0.8º. Nevertheless, the minimum first natural frequency value of 92.102 Hz was ascertained when the tapered angle was 0º. It should also be underlined that as tapered angle values go up, calculated natural frequencies exhibit climbing behavior.

In the case where the coating material is Al_2O_3, it was found out that natural frequency levels of prepared models showed an incremental trend, compared to the situation detected in Figure 6a. The highest first frequency value of 102.682 Hz and the lowest first natural frequency value of 94.322 Hz were found when the tapered angle values were 0.8° and 0° respectively (Figure 6b). Similar to the outcome seen for the models coated with AlN, it can be put forward that the first natural frequency values raised prominently from 0° to 0.8°.

When the coating layer is TiB_2 (Figure 6c), the peak value of the first natural frequency was 108.417 Hz for a 0.8° tapered angle. On the other hand, the trough value of the first natural value was determined as 100.193 Hz for the tapered angle of 0°. A parallel rising trend that was obtained for other ceramic coatings was noticed for TiB_2 coated beams depending upon the increasing tapered angle values.

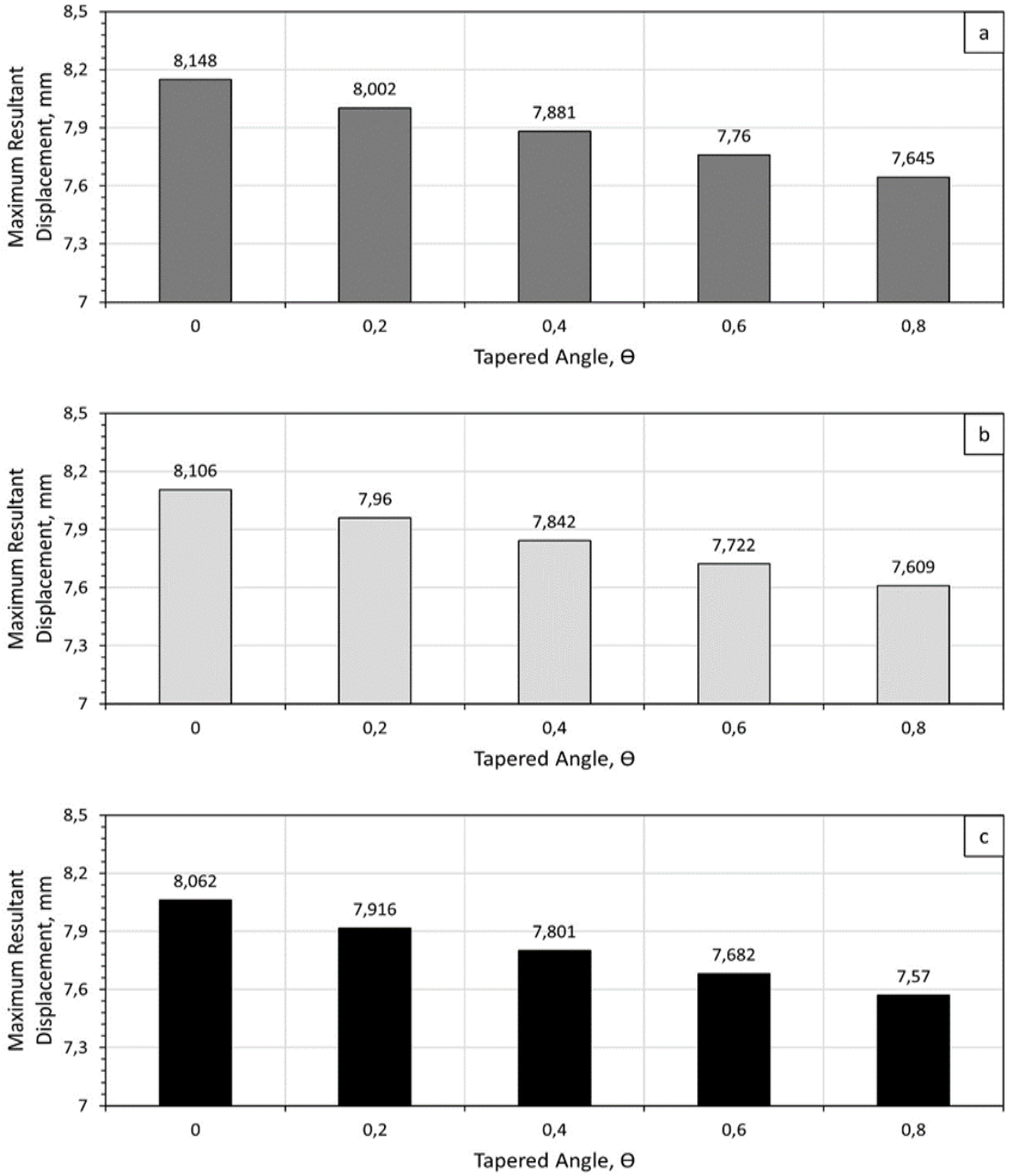

Figure 7. Maximum resultant displacement values of Ti-6Al-4V beams with different coatings depending on tapered angle for condition 2, a) AlN, b) Al_2O_3, c) TiB_2

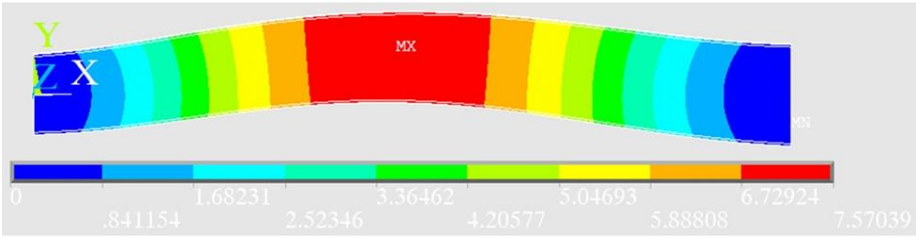

Figure 8. An illustrative example for vibrational behavior of the coated tapered beams at condition 2 (TiB_2 coated beam with tapered angle of 0.8°)

Figure 7 demonstrates the resultant displacement values of the coated models fixed at both ends according to the shifting tapered angles. Figure 7a points that the resultant displacement values descend with the rise of the tapered angle values. As a consequence of the numerical analyses, the highest and the lowest resultant displacement values were calculated as 8.148 mm and 7.57 mm for AlN and TiB_2 coated models respectively. If bar graphs shown in Figure 7a and Figure 7b are assessed together, it can be asserted that the resultant displacement values had a downward trend for Al_2O_3 coated models.

For Al_2O_3 coated models, the maximum resultant displacement value was found as 8.106 mm when the tapered angle was 0^o, and the minimum resultant displacement value was determined as 7.609 mm when the tapered angle was 0.8°. In the case where the coating material is TiB_2, a gradual diminishing was recorded in the resultant displacement values as also detected in the other two cases. From Figure 7c, the highest and lowest resultant displacement values are 8.062 mm and 7.57 mm, respectively.

Additionally, Figure 8 illustrates the simulation view of an analyzed sample, and similar behaviors were observed also for all coating types and tapered angles.

4 Conclusions

From this finite element study, the following results were obtained:

- ✓ Finite element methodology is an effective way for the determination of the natural frequency and displacement results of the hard-ceramic coated titanium alloys. Thanks to numerical analyses, lots of technical information can be attained without conducting expensive coating processes and setting up experimental equipment.
- ✓ Nitrides, oxides, and borides affect differently the natural frequency and displacement behaviors of the Ti-6Al-4V alloy. This outcome can be explicated with their different hardness and rigidity levels.
- ✓ For both fixing conditions, TiB_2 coated beams have higher first natural frequency levels than Al_2O_3 and AlN coated beams.
- ✓ For only left-side fixed condition, independently from the coating material type, taper angle influences the natural frequency results negatively, except from between 0° and 0.2°.
- ✓ For the two-sided fixing condition, as long as the taper angle values increase, the natural frequencies of the models go up irrelevant to the coating material type.
- ✓ From the data collected from the finite element analyses, it can be brought forward that there is a negative relationship between the taper angle values and resultant displacement values. This trend is valid for both fixing conditions.
- ✓ For both fixing conditions, resultant displacement levels of AlN coated beams are higher than Al_2O_3 and TiB_2 coated beams.

Conflicts of interest

No conflict of interest was declared by the authors.

Similarity rate (iThenticate): 9%

References

[1] N. Gupta, D. D. Luong and K. Cho, Magnesium Matrix Composite Foams—Density, Mechanical Properties, and Applications, Metals, 2, 238-252, 2012. https://doi.org/10.3390/met2030238.

[2] S. Ferraris and S. Spriano, Antibacterial titanium surfaces for medical implants, Materials Science and Engineering: C, 61, 965-978, 2016. https://doi.org/10.1016/j.msec.2015.12.062.

[3] J. Chen, L. Tan, X. Yu, I. P. Etim, M. Ibrahim, K. Yang, Mechanical properties of magnesium alloys for medical application: A review, Journal of the Mechanical Behavior of Biomedical Materials, 87, 68-79, 2018. https://doi.org/10.1016/j.jmbbm.2018.07.022.

[4] Ç. Bolat, İ. C. Akgün and A. Göksenli, On the Way to Real Applications: Aluminum Matrix Syntactic Foams, European Mechanical Science, 4(3), 131-141, 2020. https://doi.org/10.26701/ems.703619.

[5] V. P. Leonov, I. V. Gorynin, A. S. Kudryavtsev et al., Titanium alloys in steam turbine construction, Inorg. Mater. Appl. Res. 6, 580–590, 2015 https://doi.org/10.1134/S2075113315060076.

[6] B. Ergene, Simulation of the production of Inconel 718 and Ti6Al4V biomedical parts with different relative densities by selective laser melting (SLM) method, Journal of the Faculty of Engineering and Architecture of Gazi University, 37(1), 469-484, 2022. https://doi.org/10.17341/gazimmfd.934143.

[7] B. Ergene and B. Yalçın, A finite element study on modal analysis of lightweight pipes, Sigma Journal of Engineering and Natural Sciences, 39(3), 268-278, 2021. https://doi.org/10.14744/sigma.2021.00016.

[8] S. Liu and Y. C. Shin, Additive manufacturing of Ti6Al4V alloy: A review, Materials & Design, 164,

107552, 2019. https://doi.org/10.1016/j.matdes.2018.107552.
[9] I. Inagaki, T. Takechi, Y. Shirai and N. Ariyasu, Application and features of titanium for the aerospace industry, Nippon Steel and Sumitomo Metal Technical Report (2014), pp. 22-27.
[10] P. Singh, H. Pungotra and N.S. Kalsi, On the characteristics of titanium alloys for the aircraft applications, Mater. Today Proc., 4(8), 8971-8982, 2017. https://doi.org/10.1016/j.matpr.2017.07.249.
[11] B. Song, S. Dong, B. Zhang, H. Liao and C. Coddet, Effects of processing parameters on microstructure and mechanical property of selective laser melted Ti6Al4V, Materials & Design, 35, 120-125, 2012. https://doi.org/10.1016/j.matdes.2011.09.051.
[12] J. Alcisto, A. Enriquez, H. Garcia, Tensile Properties and Microstructures of Laser-Formed Ti-6Al-4V, J. of Materi Eng and Perform., 20, 203–212, 2011. https://doi.org/10.1007/s11665-010-9670-9.
[13] H. K. Rafi, T. L. Starr and B. E. Stucker, A comparison of the tensile, fatigue, and fracture behavior of Ti–6Al–4V and 15-5 PH stainless steel parts made by selective laser melting, Int J Adv Manuf Technol., 69, 1299–1309, 2013. https://doi.org/10.1007/s00170-013-5106-7.
[14] J. R. Zhao, F. Y. Hung, T. S. Lui, Y. L. Wu, The Relationship of Fracture Mechanism between High Temperature Tensile Mechanical Properties and Particle Erosion Resistance of Selective Laser Melting Ti-6Al-4V Alloy, Metals, 9, 501, 2019. https://doi.org/10.3390/met9050501.
[15] B. Aksakal, M. Gavgali and B. Dikici, The Effect of Coating Thickness on Corrosion Resistance of Hydroxyapatite Coated Ti6Al4V and 316L SS Implants, J. of Materi Eng and Perform., 19, 894–899 2010. https://doi.org/10.1007/s11665-009-9559-7.
[16] A. A. El Hadad, E. Peón, F. R. García-Galván, V. Barranco, J. Parra, A. Jiménez-Morales and J. C. Galván, Biocompatibility and Corrosion Protection Behaviour of Hydroxyapatite Sol-Gel-Derived Coatings on Ti6Al4V Alloy, Materials, 10, 94, 2017. https://doi.org/10.3390/ma10020094.
[17] M. F. M. Yusoff, M. R. A. Kadir, N. Iqbal, M. A. Hassan and R. Hussain, Dipcoating of poly (ε-caprolactone)/hydroxyapatite composite coating on Ti6Al4V for enhanced corrosion protection, Surface and Coatings Technology, 245, 102-107, 2014. https://doi.org/10.1016/j.surfcoat.2014.02.048.
[18] H. Asgar, K.M. Deen, Z. U. Rahman, U. H. Shah, M. A. Raza, W. Haider, Functionalized graphene oxide coating on Ti6Al4V alloy for improved biocompatibility and corrosion resistance, Materials Science and Engineering: C, 94, 920-928, 2019. https://doi.org/10.1016/j.msec.2018.10.046.
[19] B. N. Mordyuk, S. M. Voloshko, V. I. Zakiev et al. Enhanced Resistance of Ti6Al4V Alloy to High-Temperature Oxidation and Corrosion by Forming Alumina Composite Coating. J. of Materi Eng and Perform., 30, 1780–1795, 2021. https://doi.org/10.1007/s11665-021-05492-y.
[20] S. Kumar, A. Mandal, A. K. Das and A. R. Dixit, Parametric study and characterization of AlN-Ni-Ti6Al4V composite cladding on titanium alloy, Surface and Coatings Technology, 349, 37-49, 2018. https://doi.org/10.1016/j.surfcoat.2018.05.053.
[21] B. Ergene and Ç. Bolat, Determination of thermal stress and elongation on different ceramic coated Ti-6Al-4V alloy at elevated temperatures by finite element method, Sigma Journal of Engineering and Natural Sciences, 38(4), 2013-2026, 2020.
[22] N. Lin, X. Huang, X. Zhang, A. Fan, L. Qin and B. Tang, In vitro assessments on bacterial adhesion and corrosion performance of TiN coating on Ti6Al4V titanium alloy synthesized by multi-arc ion plating, Applied Surface Science, 258(18), 7047-7051, 2012. https://doi.org/10.1016/j.apsusc.2012.03.163.
[23] T. Gao, Z. Li, K. Hu, Y. Bian and X. Liu, Assessment of AlN/Mg–8Al Composites Reinforced with In Situ and/or Ex Situ AlN Particles, Materials, 14, 52, 2021. https://doi.org/10.3390/ma14010052.
[24] H. D. V. Mejia, A. M. Echavarria and G. G. Bejarano, Detailed study of the electrochemical behavior of low-reflectivity TiAlN coatings, Surface Innovations, 9(5), 296-307, 2021. https://doi.org/10.1680/jsuin.20.00079.
[25] B. Ergene and Ç. Bolat, A review on the recent investigation trends in abrasive waterjet cutting and turning of hybrid composites, Sigma Journal of Engineering and Natural Sciences, 37(3), 989-1016, 2019.
[26] Ç. Bolat, İ. C. Akgün and A. Gökşenli, Effect of aging heat treatment on compressive characteristics of bimodal aluminum syntactic foams produced by cold chamber die casting, International Journal of Metalcasting, 1-17, 2021. https://doi.org/10.1007/s40962-021-00629-0.
[27] A. Bhowmik, D. Dey and A. Biswas, Comparative Study of Microstructure, Physical and Mechanical Characterization of SiC/TiB2 Reinforced Aluminium Matrix Composite, Silicon, 13, 2003–2010, 2021. https://doi.org/10.1007/s12633-020-00591-2.
[28] S. V. Chertovskikh, L. S. Shuster and G. S. Fox-Rabinovich, Study of TiB2 Coated Hard Alloy Tool Wear Resistance During Titanium Alloy Machining, Chem Petrol Eng., 57, 690–695, 2021. https://doi.org/10.1007/s10556-021-00993-y.
[29] M. K. Thompson and J. M. Thompson, Ansys Mechanical APDL for Finite Element Analysis, Butterworth-Heinemann (Elsevier), 2017, DOI: 10.1016/B978-0-12-812981-4.00001-0.